Astron. Astrophys. 344, 607–613 (1999)

ASTRONOMY
AND
ASTROPHYSICS

The eclipse of the symbiotic star SY Muscae⋆

C.B. Pereira, V.G. Ortega, and I. Monte-Lima

Observatório Nacional, Departamento de Astronomia Galáctica e Extra-Galáctica, Rua Gen. José Cristino, 77, São Cristóvão, CEP 20921-400, Rio de Janeiro, Brazil

Received 21 August 1998 / Accepted 11 January 1999

Abstract. We present ultra-violet observations of the symbiotic star SY Mus obtained with IUE in 1996. The observations were timed to cover ingress and egress. We observe phase dependent intensity variations of the continuum and of the emission lines. These variations are caused by a wavelength dependent opacity with the characteristics of Rayleigh scattering plus a wavelength independent attenuation. From the Rayleigh scattering opacity we derive the column densities of neutral hydrogen as a function of orbital phase. We then apply inversion methods to investigate the giant's cool wind velocity profile. A new convenient analytical expression for this profile is presented and compared to other laws. The modeling of the giant's cool wind and the assumption of a terminal velocity of 30 km s^{-1}, leads to a mass loss rate of $\dot{M} \approx 1 \times 10^{-9}$ M$_\odot$ yr^{-1} for SY Mus.

Key words: stars: binaries: eclipsing – stars: binaries: symbiotic – stars: individual: SY Mus – stars: mass-loss

1. Introduction

It is well known that symbiotic stars are binary systems where eclipse effects are best seen in the spectral range covered by the IUE satellite. During the eclipse both line flux and continuum attenuation are observable as the hot companion revolves around the cool giant. The S-type symbiotics, those that have short binary periods, (1–3 years), are best suited for an analysis of eclipse effects. In addition to line and flux continuum attenuation, there is also Rayleigh scattering that introduces a strong wavelength dependent flux reduction immediately preceding and following an eclipse. It is commonly accepted that Rayleigh scattering occurs in the extended atmosphere of the cool giant, which attenuates the continuum radiation of the hot component in the far-UV range. Previous analysis of the eclipses where effects of the Rayleigh scattering are seen were done by Vogel (1991) (hereafter V91) and Vogel et al. (1992) for EG And; Pereira et al. (1995) (hereafter PVN95) for SY Mus and Pereira & Landaberry (1996) and Gonzalez-Riestra et al. (1990) for BF Cyg. The measurement of the phase dependent column densities due to Rayleigh scattering (which accounts typically for values between 10^{20}–10^{24} cm^{-2}), thus probe the density structure of the giant's wind.

In this work we concentrate on the eclipse aspect of the symbiotic phenomenon above mentioned, in order to derive, through the variation of the column density of Rayleigh scattering the most suitable empirical velocity law for the giant's cool wind. For the symbiotic star SY Mus our analysis is based on acquisition of several UV spectra obtained by the IUE satellite in the first semester of 1996. All of the data were obtained close to eclipse, just before and after the shortwave continuum attenuation. In the first part of this paper we derive the flux (emission line and continuum) phase relation and in the second part we study the structure of the wind by using velocity laws for the cool wind obtained from inversion techniques. This method was first successfully applied to EG And (V91) and a more refined approach was subsequently done by Knill et al. (1993), hereafter KDV93.

In a previous paper PVN95 analyzed all the SY Mus IUE data up to August 1992. In that work the authors derived the basic properties of the hot component (R=0.12 R$_\odot$, T=105 000 K and L=1600L$_\odot$), the nebulae as defined by the parameter X$^{H^+}$=3.3, the emission lines and continuum flux-phase relation and the ephemeris of the system which we shall adopt here (see Eq. (1)). They also derived the reddening, the nebular densities as well as the attenuation factor of the eclipse as defined by 1-Q^c(ϕ). We shall return to this point later in Sect. 3.

$$JD_{\min} = (2\,448\,922.9 \pm 2.5) + E \times (624.5 \pm 0.3) \qquad (1)$$

2. Observations

Table 1 gives the IUE observations. There are two periods of IUE observations that have not been published in previous publications: May/June 1994 and from February to July 1996.

2.1. Continuum fluxes

In Table 2 we give the observed continuum fluxes at three wavelengths where no significant emission lines are present. In the last line of Table 2, we add the fluxes at phase ϕ=0.484 taken from PVN95 as a function of the binary phase and normalized to phase 0.484. Some data points were taken from PVN95. The

Send offprint requests to: C.B. Pereira

⋆ Based on observations by the *International Ultraviolet Explorer* taken at VILSPA.

Table 1. Low resolution IUE observations of SY Mus, with exception of the spectra SWP 56975, which was observed at high resolution. Exposure times, $T_{\rm exp}$, are given in minutes. The Julian Date is given as 2 440 000+JD, the phase ϕ corresponds to the ephemeris of Eq. (1).

Date	JD	ϕ	Spectrum	$T_{\rm exp}$
15/05/94	9487	0.904	SWP 50767	8
			SWP 50768	40
			LWP 28130	12
			LWP 28131	40
26/05/94	9498	0.921	SWP 50896	8
			SWP 50897	40
			LWP 28266	40
			LWP 28267	12
04/06/94	9508	0.935	SWP 51006	8
			SWP 51007	40
			LWP 28323	12
			LWP 28324	40
15/06/94	9518	0.952	SWP 51097	8
			SWP 51098	40
			LWP 28421	12
			LWP 28422	40
06/02/96	10120	0.917	SWP 56761	10
			SWP 56762	90
			LWP 31938	35
14/02/96	10128	0.930	SWP 56805	100
			SWP 56806	10
			LWP 31985	35
23/02/96	10137	0.944	SWP 56845	10
			SWP 56846	100
			LWP 32019	35
13/04/96	10187	0.024	SWP 56973	10
			SWP 56974	150
			SWP 56975	90
			LWP 32130	39
			LWP 32131	35
25/05/96	10229	0.091	SWP 57245	10
			SWP 57250	150
			LWP 32308	35
01/06/96	10236	0.103	SWP 57312	10
			SWP 57315	150
			LWP 32324	35
04/06/96	10239	0.107	SWP 57335	10
			SWP 57336	120
			LWP 32333	35
07/06/96	10242	0.112	SWP 57356	10
			SWP 57357	100
			LWP 32349	35
11/06/96	10246	0.119	SWP 57387	10
			SWP 57388	100
			LWP 32362	35
18/06/96	10253	0.130	SWP 57417	10
			SWP 57418	80
			LWP 32370	25
23/06/96	10258	0.138	SWP 57437	10
			SWP 57438	90
			LWP 32371	35
01/07/96	10266	0.151	SWP 57473	10
07/07/96	10272	0.161	SWP 57503	90
17/07/96	10282	0.176	SWP 57551	90
			LWP 32383	35

Table 2. Observed continuum fluxes at three different wavelengths in units of 10^{-14} erg cm^{-2} sec^{-1} ang^{-1}. The phase ϕ corresponds to the ephemeris given in Eq. (1). The last line presents the continuum fluxes measured at phase 0.484 as given in PVN95.

Date	ϕ	Continuum wavelength		
		1320 [Å]	1520 [Å]	3000 [Å]
15/05/94	0.904	6.4	5.1	2.1
26/05/94	0.921	5.1	4.9	1.9
04/06/94	0.935	0.9	1.8	1.3
15/06/94	0.952	0.3	0.8	1.0
06/02/96	0.917	7.5	6.2	3.1
14/02/96	0.930	3.9	4.2	1.9
23/02/96	0.944	0.6	2.5	1.8
13/04/96	0.024	0.4	0.6	2.4
25/05/96	0.091	0.4	1.3	2.2
01/06/96	0.103	0.8	1.8	2.4
04/06/96	0.107	0.8	3.3	2.3
07/06/96	0.112	1.4	3.4	2.3
11/06/96	0.119	2.6	4.2	2.5
18/06/96	0.130	2.8	3.8	2.0
23/06/96	0.138	2.8	4.9	2.7
01/07/96	0.151	–	–	–
07/07/96	0.161	7.0	6.6	–
17/07/96	0.176	8.0	7.1	3.5
25/03/90	0.484	14.3	12.5	11.1

variation at 1320 Å and 1520 Å shows a deep minimum (flux close to zero) between the phases 0.9 and 0.1. The variation at 3000 Å differs in two aspects from the other two: the minimum flux at mid eclipse is higher and its intensity variation is less steep; the flux variations at 1320 Å and at 1520 Å indicate that the hot star is totally eclipsed whereas the flux variations at 3000 Å tell us that the nebular continuum is only partially eclipsed.

2.2. Emission lines

Tables 3 and 4 give the observed flux and Fig. 2 shows the behavior of the lines N V λ1240, O III] λ1663 and O IV], Si IV] at λ1401. In Fig. 2 they are plotted, together with the data of Table 2 of PVN95, as function of the binary phase and normalized to phase 0.484. Some data points were also taken from PVN95. The lines of C IV λ1549 and He II λ1640 are saturated in all spectra. In both IUE short (1200 Å–2000 Å) and long (2000 Å–3200 Å) wave spectra, lines of O III, N III, N IV, C III, Si III, and the blend of O IV/Si IV are also clearly present and

Table 3. Emission line fluxes observed with the SWP camera of IUE. Flux intensities are given in units of 10^{-13} erg cm^{-2} sec^{-1}. The phase ϕ corresponds to the ephemeris given by Eq. (1). The last line contains the line fluxes measured at phase 0.484 as given in PVN95.

Date	ϕ	N V 1240	O I 1304	O V 1371	O IV]* 1401	N IV] 1486	C IV 1550	[Ne V] 1575	He II 1640	O III] 1663	N IV 1718	N III] 1750	Si III] 1892	C III] 1909
15/05/94	0.904	10.3	–	2.8	13.7	8.2	42.2	2.7	48.0	14.7	–	7.3	6.0	7.0
26/05/94	0.921	7.1	–	2.1	13.6	9.3	34.7	2.2	41.9	10.0	–	5.4	4.0	6.7
04/06/94	0.935	6.1	–	1.6	13.3	8.6	36.5	–	41.2	12.0	–	4.6	4.0	6.3
15/06/94	0.952	7.6	–	2.1	13.6	7.0	34.0	1.9	45.6	10.7	–	4.7	4.6	7.1
06/02/96	0.917	10.7	–	2.9	16.5	11.4	sat	4.4	sat	11.2	1.5	6.6	4.2	9.0
14/02/96	0.930	10.5	–	2.6	16.2	7.2	sat	2.2	sat	9.5	0.3	5.9	4.3	10.3
23/02/96	0.944	9.8	–	3.0	17.7	8.9	sat	3.5	sat	12.1	0.8	5.2	5.9	9.8
13/04/96	0.024	8.0	–	2.4	18.0	8.0	sat	2.4	sat	10.6	0.8	4.7	6.1	9.6
25/05/96	0.091	7.7	–	3.0	19.2	8.5	sat	2.6	sat	11.4	0.5	5.9	7.0	9.3
01/06/96	0.103	5.4	–	1.6	12.4	5.4	sat	1.8	sat	9.1	0.4	4.4	3.8	6.6
04/06/96	0.107	8.2	–	2.5	19.4	8.7	sat	3.3	sat	10.7	1.3	6.7	6.5	9.2
07/06/96	0.112	8.4	–	2.7	21.8	9.0	sat	2.4	sat	12.5	1.3	7.0	6.8	9.9
11/06/96	0.119	8.1	–	2.9	20.5	8.4	sat	3.1	sat	12.9	0.6	6.7	6.5	10.3
18/06/96	0.130	8.2	–	2.2	20.5	11.8	sat	3.1	sat	14.6	–	7.4	7.1	11.2
23/06/96	0.138	8.9	–	2.3	21.7	9.7	sat	3.1	sat	14.4	1.2	8.2	6.3	10.6
01/07/96	0.151	–	–	–	30.7	13.2	–	–	–	17.5	–	7.6	8.3	11.4
07/07/96	0.161	13.3	–	2.7	22.3	11.9	sat	3.6	sat	15.6	1.5	7.2	6.3	10.2
17/07/96	0.176	13.5	3.7	4.9	24.1	13.4	44.1	3.8	57.0	18.7	1.8	8.3	7.2	11.6
25/03/90	0.484	127.0	32.0	8.0	90.0	47.0	sat	4.0	220.0	58.0	4.0	18.0	28.0	20.0

$*$: The O IV] $\lambda 1401$ multiplet is blended with Si IV $\lambda\lambda 1394, 1403$ resonance doublet at approximately equal strength.
sat: Saturated line.

Table 4. Emission line fluxes observed with the LWP camera of the IUE. Flux intensities are given in units of 10^{-13} erg cm^{-2} sec^{-1}. The phase ϕ corresponds to the ephemeris given in Eq. (1). The last line presents the line fluxes measured at phase 0.484 as given in PVN95.

Date	ϕ	He II 2511	He II 2733	[Mg V] 2783	Mg II 2800	[Mg V] 2929	[Ne V] 2974	O III 3133	He II 3204
15/05/94	0.904	2.7	3.1	6.5	1.5	2.6	2.0	11.7	–
26/05/94	0.921	–	2.5	6.1	–	1.9	2.1	11.5	–
04/06/94	0.935	2.1	2.7	7.4	–	1.9	1.6	11.7	–
15/06/94	0.952	2.6	2.7	7.5	–	2.1	2.3	18.3	–
06/02/96	0.917	2.9	3.4	7.6	–	2.8	1.5	13.4	8.6
14/02/96	0.930	2.4	3.8	7.0	–	2.4	1.5	11.4	7.0
23/02/96	0.944	2.7	3.3	7.6	–	1.9	1.7	10.5	–
13/04/96	0.024	3.3	3.0	8.6	–	2.0	2.4	12.8	6.7
25/05/96	0.091	2.3	3.6	7.3	–	2.2	2.4	13.3	5.7
01/06/96	0.103	2.0	2.9	9.0	–	2.3	–	14.0	9.0
04/06/96	0.107	3.2	2.9	8.7	–	2.0	–	12.0	7.6
07/06/96	0.112	2.8	3.2	9.0	–	3.0	3.0	13.5	5.9
11/06/96	0.119	3.9	3.2	9.0	–	2.1	2.1	14.0	6.9
18/06/96	0.130	2.9	2.9	8.1	–	3.5	2.6	10.6	7.3
23/06/96	0.138	3.2	3.6	9.0	–	2.4	2.7	14.4	7.8
17/07/96	0.176	3.7	5.0	10.5	3.5	4.5	3.9	17.4	11.1
25/03/90	0.484	12.0	6.0	11.0	27.0	6.0	4.0	53.0	15.0

their fluxes can be reliably measured. The same applies to He II, Mg II, Mg V, and O III in the long wavelength spectra.

As well as the continuum fluxes, the emission lines fluxes are clearly phase dependent. Fig. 2 depicts the bevavior for the lines N Vλ1240, O III]λ1663 and O IV]λ1401. Contrary to the continuum fluxes at 1320 Å and at 1520 Å, the emission lines are partially eclipsed.

3. The eclipse

In PVN95, it was shown that the shape of the continuum exhibits large differences when spectra are taken few months apart. In their Fig. 1, the continuum shortwards of 1500 Å shows strong extinction due to Rayleigh scattering (see Isliker et al., 1989). If Rayleigh scattering were the only source responsible for the

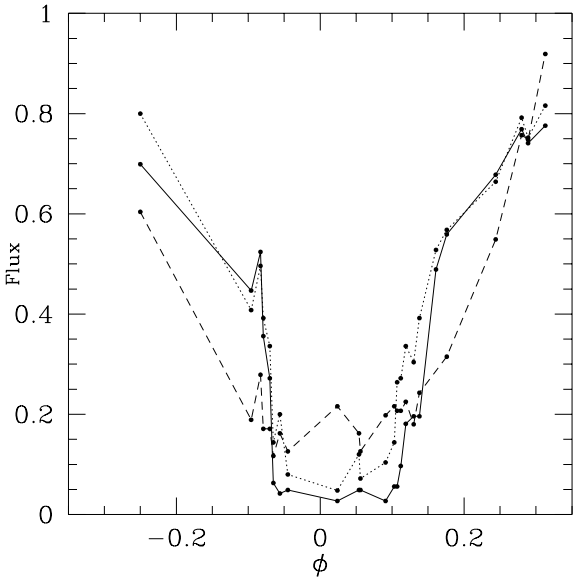

Fig. 1. Phase dependence of the continuum fluxes. Fluxes at 1320 Å (solid lines), 1520 Å (dotted lines) and at 3000 Å (dashed lines) were normalized to phase ϕ=0.484 and are given as function of phase ϕ.

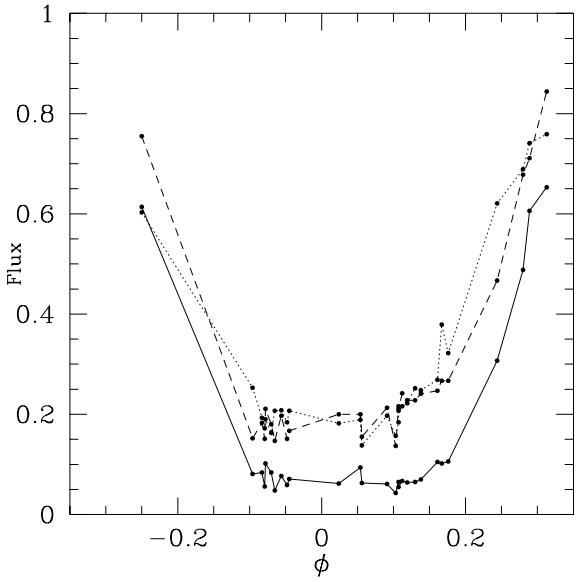

Fig. 2. Phase dependence of some emission line fluxes. Fluxes for the lines N Vλ1240 (solid lines), O III]λ1663 (dotted lines) and O IV]λ1401 (dashed lines) were normalized to phase ϕ=0.484 and are given as function of phase ϕ.

Table 5. Column densities of neutral hydrogen, N_H, and continuum attenuation factors 1-Q^c, for various phases ϕ. The attenuation factors 1-Q^c are given for the stellar and nebular components.

ϕ	N_H (cm^{-2})	stellar	nebular
0.917	3.0×10^{21}	0.53	0.20
0.930	3.0×10^{22}	0.39	0.12
0.944	4.0×10^{23}	0.21	0.15
0.091	1.0×10^{24}	0.09	0.23
0.107	3.0×10^{23}	0.14	0.24
0.119	1.5×10^{23}	0.38	0.18
0.130	9.0×10^{22}	0.45	0.18
0.161	3.0×10^{21}	0.65	–
0.176	$< 1.0\times10^{21}$	0.63	0.22

attenuation of the continuum flux shortwards 1500 Å, the observed spectrum could be fitted by the expression,

$$F_\lambda(\phi) = F^0_\lambda \cdot e^{-N_H(\phi)\sigma^R_\lambda} \quad (2)$$

where σ^R_λ represents the wavelength dependent Rayleigh cross section, and F^0_λ is the unattenuated black-body continuum flux of the source with the parameters R=0.12 R$_\odot$ and T=105 000 K.

However, as it was demonstrated by PVN95, there is an additional wavelength independent attenuation, which can be expressed in terms of the relation

$$F_\lambda(\phi) = F^0_\lambda \cdot (1 - Q^c(\phi)) \cdot e^{-N_H(\phi)\sigma^R_\lambda} \quad (3)$$

where Q^c(ϕ) is the additional phase dependent attenuation. In Table 5 we list for the eclipse observations the values of the attenuation factor for the stellar and nebular components and the column densities of Rayleigh scattering, N_H.

The new ultra-violet observations of SY Mus analyzed in this paper are the first that well cover the phases close the total eclipse of the hot star. Inspecting Table 1, it is apparent that the observations were performed in order to also probe the extinction of the shortwave continuum between 1200 Å and 1500 Å where the effects of Rayleigh scattering should be present. This is indeed the case as demonstrated by the values of the column densities given in Table 5. However, there is an asymmetry of the values of the column densities derived before and after the total eclipse. This is better seen in a plot of N_H $versus$ $\tilde{\phi}$, where $\tilde{\phi}$ is the reduced phase as defined in V91, (Fig. 3).

The asymmetry of the observed column densities may reflect a situation in which the distribution of the neutral hydrogen is not symmetric around the cool star. The erratic behavior of the emission lines close to the eclipse (see Fig. 2) might be a further indication of a region with complex structure. An alternative explanation for the observed asymmetry of the column density is that the ephemeris should have corrections. Notwithstanding our observations do not allow us to precise the instant of minimum, the observed asymmetry of the column densities suggests a negative phase shift of 0.035 to the observed phases. This change is smaller than what was previously determined in PVN95, when the phase was corrected at about 0.08 positive from Kenyon & Bateson (1984) ephemeris. This small phase shift is enough to allow the study of the giant's cool wind on the basis of the observed hydrogen column densities.

An argument for phase shifting would come if we analyzed only the egress data. Inspecting Fig. 3(a), we notice that at the reduced phase $\tilde{\phi}$=0.09 the total eclipse would be still in progress. From Eq. (6) below, this would result in the very unlikely situation of total eclipse occurrence at an impact parameter of b=2.33 giant's stellar radii. Aside from that, the analysis of only the egress data, using formula (7) below, would indicate a wind velocity of only 1% of the terminal velocity at the distance of

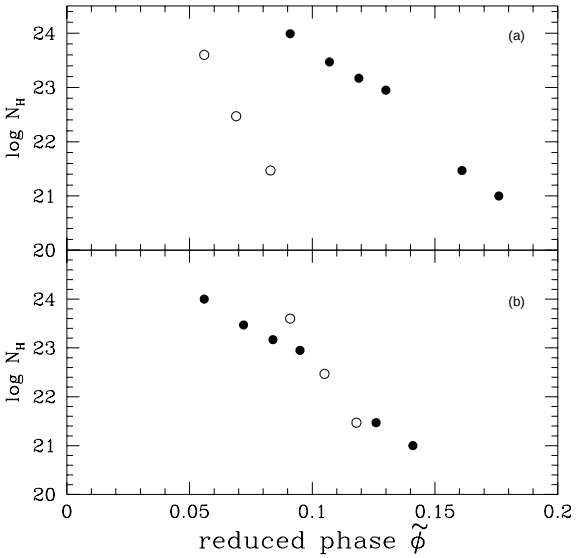

Fig. 3a and b. Observed column densities of SY Mus plotted against the reduced phase as defined in Vogel (1991) **a**. In **b** the reduced phases were corrected by 0.035. The open circles represent the points at phases 0.944, 0.930 and 0.917 and the filled circles the points at phases 0.091, 0.107, 0.119, 0.130, 0.161 and 0.176.

6.0 cool giant's stellar radii. Such an analysis would lead further to an extremely low mass-loss rate of the order of 10^{-13} $M_\odot$/yr assuming a wind terminal velocity of 30 km s^{-1}.

4. The wind structure of SY Mus

The column densities of neutral hydrogen determined as function of the orbital phase from the observed spectra, allow to investigate the cool wind structure of the giant component. This was first shown by V91 in a pioneer study of the symbiotic binary EG And. The analysis of the observed column densities led Vogel to determine an empirical velocity law for the cool wind in that system. The law turned out to be remarkable different from the "β-laws" usually employed to describe stellar winds. In fact, it is characterized by low velocity values near the giant component followed by a very rapid increase at a distance of approximately 3 giant's stellar radii. The emission lines in the UV spectra of SY Mus are evidence that some portion of the giant's stellar wind is ionized by the radiation stemming from the hot component. The modeling of EG And by V91 indicated nevertheless that the assumption of wind neutrality is a fairly good first approximation for the study of the red giant's wind. Assuming further that the wind is spherically symmetric and that the eccentricity of the system is negligible (Schmutz et al., 1994) one can write for the column density

$$N_H(b) = a \int_b^\infty \frac{dr}{\sqrt{r^2 - b^2}\, r\, v(r)} \tag{4}$$

where b is the impact parameter, or projected separation between the components, and $v(r)$ is the wind velocity at distance r from the giant's center. In this equation b and r are adimensional quantities, expressed in units of the giant's radius R. Similarly the velocity $v(r)$ is expressed in units of the terminal velocity v_∞. The dimension of the parameter a, also called parameter of the system, given by

$$a = \frac{2\ \dot{M}}{4\,\pi\,\mu\,m_H\,R\,v_\infty} \tag{5}$$

where $\dot{M}$ is the mass-loss rate of the red giant and μm_H is the average molecular weight, determines therefore the physical dimensions of the hydrogen column density, N_H(b).

The impact parameter, b, is related to the inclination angle i of the orbital plane and the phase ϕ by the formula

$$b^2 = p^2\,(cos^2 i\ +\ sin^2\phi\, sin^2 i) \tag{6}$$

p being the separation (in units of R) between the components of the binary. For SY Mus we employ p=4.3 (Schmutz et al., 1994) and i=95.8 (Harries & Howarth, 1996a). In order to find the velocity $v(r)$ from the observed column densities N_H(b), Eq. (4) has to be inverted. This is an integral equation of Fredholm's type but it can be brought to Abel's type by means of suitable transformations. Such inversion problems are frequently ill-posed and demand special methods for their investigation. Specifically, the empirical determination of stellar wind velocity by means of Eq. (4) has been discussed by Kessler (1991) and KDV93 who have developed procedures for its inversion. In Kessler (1991) the sought-for function (the "source function") is approximated by a piecewise linear function and the velocity computed numerically for each value of the column density (the "data function"). In KDV93 the inversion is accomplished through explicit diagonalization of the Abel's operator. In this method the "data function" is represented by a Taylor expansion and the velocity field is then obtained from the inverted Abel's operator. We shall employ both approaches to determine the cool wind velocity profile of SY Mus and the resulting column densities to be compared with the observations.

For the velocity obtained from the numerical inversion of the observed column densities we have found that a convenient analytical description is provided by the expression

$$v(r)/v_\infty = \frac{\gamma(A, B(r-1))\ +\ A\, e^{-B\,r}\,\gamma(A, Br)}{\Gamma(A)} \tag{7}$$

where Γ and γ are the complete and incomplete gamma functions respectively and are given by

$$\Gamma(A) = \int_0^\infty t^{A-1}\, e^{-t}\, dt \tag{8}$$

and

$$\gamma(A, r) = \int_0^r t^{A-1}\, e^{-t}\, dt \tag{9}$$

For a fixed value of the parameter of the system a, the parameters A and B in Eq. (7) can be chosen so as to obtain the best description of the velocity. The parameters A and B fix also the coordinates (r_0, v_0) of the inflection point:

$$r_0 = \frac{A\ -\ 1}{B} + 1 \tag{10}$$

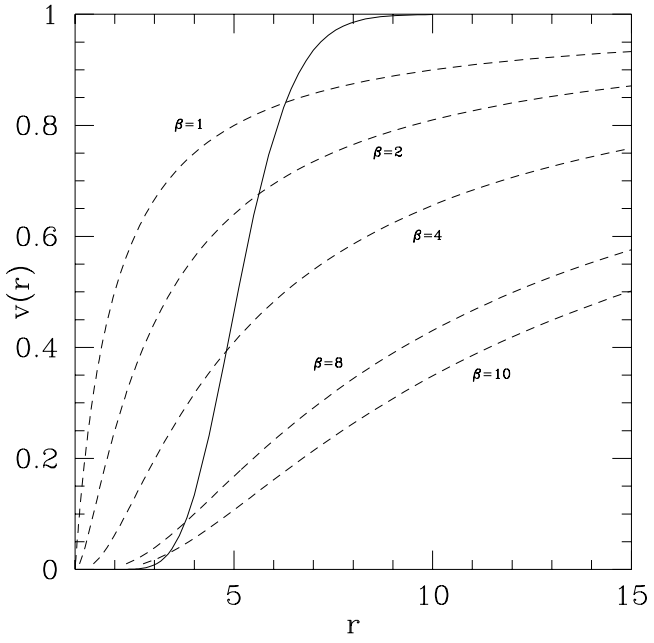

Fig. 4. Wind velocity profile from Eq. (7) with A=14.2 and B=3.383 (solid line). Some profiles according to the β-law (dashed lines) are also shown for comparison.

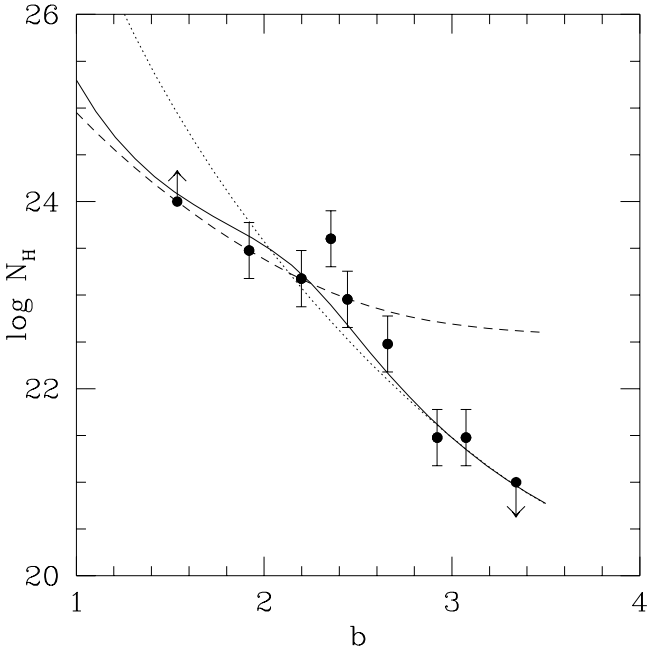

Fig. 5. Observed column densities as a function of the impact parameter. The curve represents the computed column densities using the velocity profile given formula (7) (solid line), using Vogel's law (dotted line) and using formula (13) (dashed line).

$$v_0 = \frac{\gamma\,(A, A-1)}{\Gamma(A)} \tag{11}$$

In Fig. 4 we show the velocity profile obtained in this way with A=14.20 and B=3.383. Of course, it must be remembered that this behavior is an extrapolation due to the adopted form of the function and to its fitting to the observed points in the region $b < 3.5$.

With the value a=2×10^{20} cm^{-2} of the parameter of the system, this law translates in column densities which best match the observations (Fig. 5).

We have compared the column densities furnished by the velocity profile (Eq. 7) with those resulting from Vogel's law (V91), first applied to investigate the wind structure of the symbiotic system EG And,

$$v(r)/v_\infty = \begin{cases} c_1\,(r/R)^m & \text{for r/R} \le \text{r}_0 \\ 1 - e^{-c_2(r/R - c_3)} & \text{for r/R} > \text{r}_0 \end{cases} \tag{12}$$

In Fig. 5, we plot the column densities implied by Vogel's function with parameters m=11, r$_0$=3.75, v$_0$=0.2 and a=4×10^{20} cm^{-2}.

The agreement between the curves is quite good particularly for large values of impact parameter where they practically coincide.

Following KDV93 we consider now the finite Taylor expansion

$$N_H(b) = \sum_{i=1}^{N} \frac{N_i}{b^i} \tag{13}$$

and best-fit this expression to the observed data. The inversion method of KDV93 permits then to invert the Abel's operator and to determine the corresponding Taylor expansion for the "source function" from which the velocity field can be reconstructed. We remark however, that the column density is a decreasing function of the impact parameter b, asymptotically tending to the value $a\pi/2b$ which implies a non-decreasing velocity profile converging to a constant terminal value. The Knill method requires that the observational points cover all the region until this terminal value is reached, in order to avoid a random behavior of the polynomial outside this observational region. This is not our case, in view of the restricted range of the observations. In fact we did not find any best-fitting polynomial through all the points and having at the same time the required behavior of the wind velocity profile. Neverthelees, including in the fitting only those points giving such a behavior we can get an upper bound for the parameter a. The polynomial (N=4) that we obtained fits the four inner points plus the point at b=2.658 with the lowest possible value of N$_{\rm H}$ that guarantees that the polymonial does not have any positive root. This polynomial is shown in Fig. 5 and the bound given by it is a=6.0×10^{20} cm^{-2}.

The relation 5 shows that the parameter of the system a is related to important physical quantities such as the wind terminal velocity, v$_\infty$ and the mass-loss rate $\dot{M}$ of the red giant. Assuming a wind terminal velocity v$_\infty$=30 km s^{-1}, a giant radius of 86 R$_\odot$ (Schmutz et al., 1994) and making use of the values of the parameter a from our modeling, we obtain for the mass-loss rate: $\dot{M}$=0.83×10^{-9} M$_\odot$/yr for the velocity profile given by expression (7); $\dot{M}$=1.7×10^{-9} M$_\odot$/yr for Vogel's law as applied to SY Mus. The upper limit of the parameter a results in the bound $\dot{M}$=2.5×10^{-9} M$_\odot$/yr for the mass-loss rate. The

models by Harries & Howarth (1996) of Raman scattering in symbiotic stars suggest a terminal velocity of about 60 km s^{-1} for SY Mus. This would give $\dot{M}$=1.6×10^{-9} M$_{\odot}$/yr if we use formula (7). We notice that for the assumed terminal velocities the estimated the mass-loss rate is rather low if compared with most of the S-type symbiotic systems with radio measurements (see Seaquist & Taylor 1990). This is especially the case for the first two models from which it was possible to obtain simultaneously an estimate of the parameter a and a good matching of the observed neutral hydrogen column densities.

5. Conclusions

In this paper we presented new spectroscopic observations of the eclipsing symbiotic system SY Mus. The observations, done by IUE satellite, cover phase intervals before and after the total eclipse of the hot star. We obtained phase dependent flux for emission lines and continuum points where no significant emission lines were present. We also derived from the observations close to the eclipse the column densities of Rayleigh scattering.

Using the eclipse observations of hydrogen column densities we modeled the giant's cool wind velocity assuming neutrality as a first approximation. The velocity is reasonably well described by the empirical law given by Eq. (7). Probably this function is well adapted for modeling the neutral wind of other S-type symbiotic systems. The estimated mass-loss rate from the giant in SY Mus turned out to be lower than for most S-type systems with mass-loss rates derived from radio observations. This refers not only to our model given by Eq. (7) but also to the results from the application of Vogel's empirical law (V91) and the method developed by KDV93.

As pointed out before, our analysis assumes neutrality for the stellar wind. The column densities fall quite quickly near b=3. We cannot exclude the possibility that the ionization front of the hydrogen is exerting some influence in that range of the impact parameter. The modelling of the front could in principle set further constraints on the parameter a and therefore on the mass-loss rate of SY Mus.

Acknowledgements. C.B.P thanks the travel support from CNPq – Brazil under grant 450621/96 and FAPERJ under grant E-26/150.398/96. We thank Dr S. Junqueira for help with SM package. We thank the staff at Vilspa for taking the IUE spectra of SY Mus for the key project SI067. In particular we appreciate the efforts of our contact RAs Drs. Domitilla de Martino and Heinz Andernach. We thank Dr W. Schmutz for his helpful comments. We also thank the referee, Dr Ian Howarth, for valuable remarks and comments.

References

Gonzalez-Riestra R., Cassatela A., Fernandez-Castro T., 1990, A&A 237, 385
Harries T.J., Howarth I.D., 1996a, A&A 310, 235
Harries T.J., Howarth I.D., 1996, A&AS 119, 61
Isliker H., Nussbaumer H., Vogel M., 1989, A&A 219, 271
Kenyon S.J., Bateson F.M., 1984, PASP 96, 321
Kessler T., 1991, Diplomarbeit, ETH-Zürich
Knill O., Dgani R., Vogel M., 1993, A&A 274, 1002, (KDV93)
Pereira C.B., Vogel M., Nussbaumer H., 1995, A&A 293, 783, (PVN95)
Pereira C.B., Landaberry S.J.C., 1996, AJ 111, 1329
Seaquist E.R., Taylor A.R., 1990, ApJ 349, 313
Schmutz W., Schild H., Mürset U., Schmid H.M., 1994, A&A 288, 819
Vogel M., 1991, A&A 249, 173, (V91)
Vogel M., Nussbaumer H., Monier R., 1992, A&A 260, 156